$1s\sigma 2s\sigma^3\Sigma_g \rightarrow 1s\sigma 2p\sigma^3\Sigma_u$ transition, with atomic lines also visible. Decay of the molecular spectrum is so rapid that it cannot be photographed within the 10–15-μsec resolution of our shutter. The light at times from 0–600 μsec is continuous in character, having a maximum at about 4250A and cutting off at about 3400A; and is thus not identifiable with the molecular continuum. Changes in spectral distribution and absolute intensity are observed in passing from quartz to Pyrex containers.

Estimates to within a factor of 2 or 3 (by means of a calibrated 1P28 photo-tube) of the absolute energy lying in the band of the 1P28 per disappearing electron lead to results which (a) are less than 1/500 of the available energy (ionization potential) per recombining electron, and (b) vary widely with time instead of remaining constant. These and other results lead to the conclusion that the light associated with the hydrogen afterglow arises from the container walls, and that nonradiatiative volume recombination accounts for the removal of electrons. A possible mechanism is

$$H_2^+ + e \rightarrow H + H + \text{K.E.},$$

with the $1s\sigma 2p\sigma^3\Sigma_u$ or similar state as the final state of the molecule.

* This research was supported in part by the ONR.
† AEC Predoctoral Fellow.
[1] Holt, Richardson, Howland, and McClure, Phys. Rev. **77**, 239 (1950).
[2] M. A. Biondi, Phys. Rev. **79**, 733 (1950).

Californium Isotopes from Bombardment of Uranium with Carbon Ions*

A. Ghiorso, S. G. Thompson, K. Street, Jr., and G. T. Seaborg
Radiation Laboratory and Department of Chemistry, University of California, Berkeley, California
November 8, 1950

THE recent production and identification[1] of isotopes of elements with atomic numbers up to six higher than the target element through bombardment with approximately 120-Mev carbon (+6) ions made it seem worth while to apply this technique to the transuranium region.

Accordingly, small pieces of natural uranium metal (about 0.5 mil thick and 2.5 cm by 0.6 cm area) were irradiated in the internal carbon ion beam in the Berkeley 60-inch cyclotron. Following the irradiations, the uranium was dissolved in dilute hydrochloric acid containing hydrogen peroxide and a transplutonium fraction was isolated through the use of lanthanum fluoride and lanthanum hydroxide precipitation steps followed by the ion exchange adsorption column procedure, in which concentrated hydrochloric acid is used to separate the tripositive actinide elements from the rare earth elements.[2]

The transplutonium fractions in hydrochloric acid were evaporated as weightless films on platinum plates which were placed in the ionization chamber of the 48-channel pulse analyzer apparatus in order to measure the yield and energies of any alpha-particles which might be present. In the best experiment at about one hour after the end of the 90-min bombardment, some 50 disintegrations per minute of the distinctive 7.15±0.05-Mev alpha-particles[3] of Cf^{244} were observed to be present and to decay with the 45-min half-life. The Cf^{244} was presumably formed by the reaction $U^{238}(C^{12}, 6n)$.

After the decay of the alpha-particles due to Cf^{244}, about five disintegrations per minute of alpha-particles with 6.75±0.05-Mev energy were observed and this alpha-radioactivity decayed with a half-life of about 35 hours. In subsequent experiments involving the use of an ion exchange method[4] to separate the individual actinides from each other, both the ~45-min and ~35-hour activities were found together in the chemical fraction corresponding to the new element californium. A consideration of the systematics of alpha-radioactivity[5] leads us to the view that this 35-hour period is due to the new isotope Cf^{246} formed by the reaction $U^{238}(C^{12}, 4n)$. The measured half-life agrees with the expected alpha half-life for the observed energy for an even-even isotope of the element with atomic number 98.

It is not possible at this time to obtain a good estimate of the intensity of the carbon ion beam. Therefore, the cross sections for the reactions given above cannot be calculated. However, it is interesting to note that the indicated yields for the (C, $6n$) and (C, $4n$) reactions are comparable.

If the mass assignment of the new 35-hour activity to Cf^{246} is correct, these new data give a better idea as to the slope of the alpha-energy *vs* mass number line for californium, which in turn makes it possible to make better predictions of the radioactive properties of the nuclides in this region.

We wish to express our appreciation to Professor J. G. Hamilton, J. F. Miller, G. B. Rossi, T. M. Putnam, Jr., M. T. Webb, and the operating crew of the 60-inch cyclotron in the Crocker Laboratory for their help in the carbon ion bombardments. We would also like to thank Mr. E. K. Hulet for his help in the chemical separations.

* This work was performed under the auspices of the U. S. AEC.
[1] Miller, Hamilton, Putnam, Haymond, and Rossi, Phys. Rev. **80**, 486 (1950).
[2] K. Street, Jr. and G. T. Seaborg, J. Am. Chem. Soc. **72**, 2790 (1950).
[3] Thompson, Street, Jr., Ghiorso, and Seaborg, Phys. Rev. **78**, 298 (1950).
[4] Thompson, Street, Jr., Ghiorso, and Seaborg, Phys. Rev. **80**, 792 (1950).
[5] Perlman, Ghiorso, and Seaborg, Phys. Rev. **77**, 26 (1950).

Thresholds of Photo-Neutron Reactions*

R. Sher, J. Halpern, and W. E. Stephens
Randal Morgan Laboratory of Physics, University of Pennsylvania Philadelphia, Pennsylvania
November 6, 1950

NEUTRON yields as functions of the maximum energy of the bremsstrahlung output of the University of Pennsylvania betatron have been measured for several substances in the energy region from threshold to 22 Mev. The samples, of the order of 50 grams of high purity materials, were inserted in a block of paraffin 9 in×9 in×20 in, in which was also placed a $B^{10}F_3$ counter (Fig. 1). Shielding against background neutrons was obtained by surrounding the apparatus with sheet cadmium, then with about 4 inches of paraffin mixed with B_4C, then with about 1 foot of additional paraffin. The samples were $\frac{3}{4}$-in diameter cylinders. The collimated x-ray beam was about $\frac{5}{8}$ in diameter and irradiated the samples axially. The distance from sample to betatron target was 8.5 feet. The counter was parallel to the beam and about one inch away.

In order to avoid counting pile-up due to the x-ray pulse, and also to avoid being bothered by transient effects on the counting system due to the x-ray burst and auxiliary betatron pulses, only those neutrons were counted which, having been delayed in the paraffin, entered the counter some time after each burst of x-rays. This was done by constructing an electronic gate signal which was delayed from each x-ray burst by about 30 μsec, and whose dura-

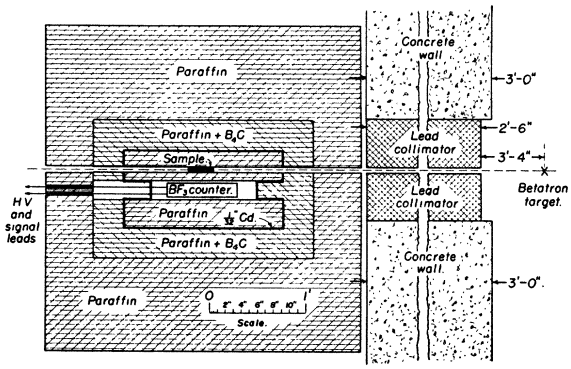

FIG. 1. Schematic diagram of the experimental arrangement (side view).

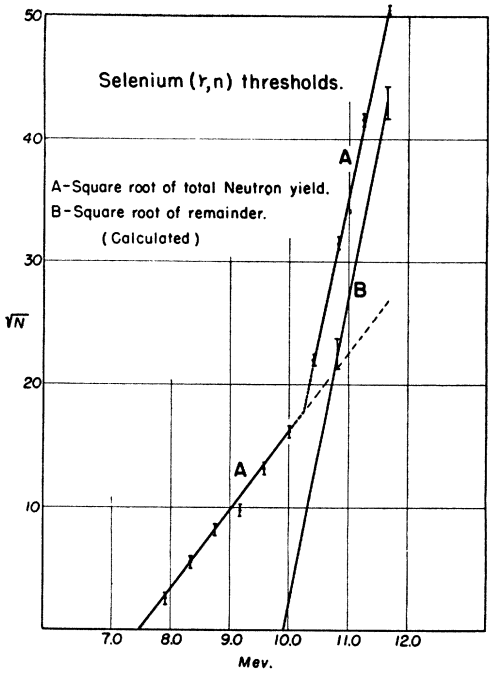

FIG. 2. Square root of neutron yield *vs* energy. This graph is a typical case in which two thresholds are present: Se^{77} (7.5 Mev) and $Se^{82(?)}$ (9.9 Mev).

tion was about 300 μsec. (The time between x-ray pulses was 5550 μsec.) The gate was "counted" in coincidence with the pulses from the BF_3 chamber; thus, only those neutrons which fell within the gated interval were recorded.

The maximum energy of the x-ray beam was varied by expanding the electron beam in the betatron at any desired value of the magnetic field, using circuits similar to those described by Katz, *et al.*[1] The energy scale was calibrated using the deuterium photodisintegration threshold at 2.23 Mev, the $Cu^{63}(\gamma, n)Cu^{62}$ threshold at 10.9 Mev, and the $C^{12}(\gamma, n)C^{11}$ threshold at 18.7 Mev.

Thresholds were determined by plotting the square root of the neutron yield as a function of energy in the region around threshold.[2] The resulting graphs are of two kinds: those in which one straight line is obtained, characteristic of substances containing contributions of only one isotope, and those in which one or more abrupt increases in slope occur, corresponding to the additional contributions of isotopes with higher thresholds (Fig. 2). In this case the yields corresponding to the lower thresholds were extrapolated and subtracted from the total yield, and the higher thresholds obtained by plotting the square root of the remainder.

TABLE I. Photo-neutron thresholds.

Parent isotope	Threshold (Mev)[a]	Parent isotope	Threshold (Mev)[a]
$_5B^{10}$	7.6	$_{38}Sr^{88}$	10.9
$_5B^{11}$	11.1	$_{41}Nb^{93}$	8.7
$_{11}Na^{23}$	12.6	$_{46}Pd^{105}$	7.2
$_{12}Mg^{25}$	7.1	$_{46}Pd^{?}$	8.8
$_{12}Mg^{26}$	10.1±1.0	$_{52}Te^{125}$	6.8
$_{14}Si^{29}$	8.4	$_{52}Te^{?}$	8.8
$_{16}S^{34(?)}$	10.8	$_{55}Cs^{133}$	9.0
$_{22}Ti^{49}$	8.7	$_{56}Ba^{137}$	7.1
$_{22}Ti^{48(?)}$	11.6	$_{56}Ba^{138(?)}$	8.7
$_{23}V^{51}$	10.8±0.5	$_{57}La^{139}$	8.8
$_{24}Cr^{53}$	7.5	$_{58}Ce^{?}$	6.7
$_{24}Cr^{52}$	11.6±0.4	$_{58}Ce^{?}$	8.7
$_{27}Co^{59}$	10.0	$_{74}W^{183}$	6.0
$_{28}Ni^{61(?)}$	7.5	$_{74}W^{?}$	7.1
$_{34}Se^{77}$	7.5	$_{74}W^{?}$	9.5
$_{38}Sr^{87}$	7.2±0.5		

[a] ±0.3 Mev unless otherwise indicated.

The advantage of detecting neutrons rather than residual radioactivities is, of course, the possibility of finding (γ, n) processes whose products are either stable or have very long or very short half-lives. One also may obtain by this method neutrons generated by other processes such as $(\gamma, 2n)$, (γ, np), etc. The thresholds for these reactions generally lie considerably higher than (γ, n) thresholds, however, and so their presence will have no effect on the present results, but will be advantageous in interpreting the total yield data. On the other hand, the identification of some of the isotopes becomes more doubtful. For a nucleus of even Z, the lowest threshold was assumed to be that of the isotope of highest odd A. Higher thresholds were occasionally assigned on the basis of isotopic abundance; in such substances as Pd, Te, and W, there are several even A isotopes of almost equal abundance and identification was not possible.

The results are listed in Table I. The experimental errors are ±0.3 Mev unless otherwise indicated.

In addition to the new thresholds listed in the table, more than twenty thresholds were observed which had been previously reported.[2-4] These agreed with the earlier results within experimental error.

The yield data will permit a detailed study of the cross sections of photo-neutron processes and their variation with energy; this work and more complete details about the experiment will be reported at a later date.

* Assisted by the joint program of the AEC and ONR.

[1] Katz, McNamara, Forsyth, Haslam, and Johns, Can. J. Research **A28**, 113 (1950).
[2] McElhinney, Hansen, Becker, Duffield, and Diven, Phys. Rev. **75**, 542 (1949).
[3] Hansen, Duffield, Knight, Diven, and Palersky, Phys. Rev. **76**, 578 (1949).
[4] W. E. Ogle and R. E. England, Phys. Rev. **78**, 63 (1950); Ogle, Brown, and Carson, Phys. Rev. **78**, 63 (1950); G. C. Baldwin and H. W. Koch, Phys. Rev. **67**, 1 (1945).

Kramers' Theorem and Nuclear Effects in Paramagnetic Absorption*

C. KIKUCHI†
Brookhaven National Laboratory, Upton, New York
November 6, 1950

SHORTLY after the discovery of the hfs in solids by Penrose,[1] Pryce[2] pointed out a relationship between ΔH, the hfs component separation for the cobalt ion, and θ, the angle between the crystalline axis and the applied magnetic field. Later Ingram[3] showed that this same relation applies to the copper ion. It occurred to us, therefore, to investigate the conditions under which Pryce's relation would be valid. We should like to point out that his relation is a consequence of Kramers' theorem,[4] when the effect of the nuclear magnetic moment is taken into account to the first approximation.

Let ψ_1 and ψ_2 be the wave functions of a doubly degenerate electron ground state of a paramagnetic ion. In the presence of a magnetic field, the degeneracy will be removed and the wave functions of the two states become

$$f_{\frac{1}{2}}=[g_\perp \sin\theta\psi_1+(g-g_{11}\cos\theta)\psi_2]/[2g(g-g_{11}\cos\theta)]^{\frac{1}{2}}, \quad (1)$$

$$f_{-\frac{1}{2}}=[-(g-g_{11}\cos\theta)\psi_1+g_\perp \sin\theta\psi_2]/[2g(g-g_{11}\cos\theta)]^{\frac{1}{2}}, \quad (2)$$

corresponding to the magnetic energies $\frac{1}{2}\mu_B g H$ and $-\frac{1}{2}\mu_B g H$. Here g is given by $(g_{11}^2\cos^2\theta+g_\perp^2\sin^2\theta)^{\frac{1}{2}}$. The quantities g_{11} and $g_\perp$ will depend, of course, on the particular ion and the crystalline electric field; but the form of the wave functions as given above will be the same for any ion. The invariance requirement leads to the following expression for the nuclear interaction potential:

$$V=a_1\mathbf{L}\cdot\mathbf{I}+a_2[(3\mathbf{I}\cdot\mathbf{r}\mathbf{S}\cdot\mathbf{r}/r^2)-(\mathbf{I}\cdot\mathbf{S})]+a_3\mathbf{I}\cdot\mathbf{S}. \quad (3)$$

If J is a good quantum number, the above interaction potential can be expressed in the form $a_J\mathbf{I}\cdot\mathbf{J}$. In addition, there is the term